Nanostructurated Complexes of Poly(β,L-malate) and Cationic Surfactants: Synthesis, Characterization and Structural Aspects

José A. Portilla-Arias,† Montserrat García-Alvarez,† Antxon Martínez de Ilarduya,† Eggerhard Holler,‡ and Sebastián Muñoz-Guerra*,†

Departament d'Enginyeria Química, Universitat Politècnica de Catalunya ETSEIB, Diagonal, 647, 08028 Barcelona, Spain, and Institut für Biophysik und Physikalische Biochemie der Universität D-93040, Regensburg, Germany

Received July 12, 2005; Revised Manuscript Received October 14, 2005

Ionic complexes of microbially produced poly(β,L-malic acid) and alkyltrimethylammonium surfactants with linear alkyl chains containing even numbers of carbon atoms from 14 up to 22, were investigated. Complexes with a stoichiometric or nearly stoichiometric composition were prepared by precipitation from equimolar mixtures of aqueous solutions of the two components. All complexes were found to adopt supramolecular stratified structures made of alternating layers of poly(β,L-malate) and surfactant with a periodicity on the length scale of 3−5 nm, which increased proportionally to the length of the polymethylene chain. In these complexes, alkyl side chains with more than 16 carbon atoms were partially crystallized showing reversible melting at temperatures between 40 and 70 °C. After melting, a smectic LC phase that isotropicized at ∼100 °C was observed for all of the complexes. Conformational and dimensional changes taking place in the complexes by effect of heating were analyzed by ^{13}C CP-MAS NMR and powder X-ray diffraction.

Introduction

The self-assembly of matter on the nanometric scale is continuously manifested throughout biotic and abiotic nature, and it is accepted to be the cornerstone of synthetic routes leading to nanostructured materials.[1] Both block and comblike polymers constituted by units of different chemical natures are the system of choice for the construction of ordered polymeric nanostructures.[2] Other preferred strategies are based in the coupling of counterparts by noncovalent interactions as hydrogen-bonding[3] or ionic complexation.[4] The two basic building blocks commonly used for the preparation of ionic polymeric complexes are polyelectrolytes and ionic surfactants of opposite charges. The polyelectrolyte−surfactant complexes are spontaneously generated when aqueous solutions of the two components are mixed, and once formed, they remain stable due to favorable electrostatic interactions. The method constitutes an elegant and effective tool for the preparation of nanoestructurated systems that otherwise should imply laborious and time-consuming manipulations.

Comblike polymeric systems bearing linear alkyl side chains are very prone to be arranged in biphasic layered structures in which the main chain and the side chain alternate with a periodicity on the nanometric scale.[5] About 10 years ago, Antonietti et al.[6] demonstrated that poly(styrene sulfonate)−alkyltrimethylammonium complexes showed well-defined solid-state structures which are based on new amphotropic polyelectrolyte-surfactant phases. As recently reviewed by Thünemann,[4] a variety of comblike polyelectrolyte-surfactant complexes of chemosynthetic nature have been investigated for their scientific and technological interest, and the methodology for their characterization and property evaluation is well settled today. A second family is that constituted by complexes made of peptidic polyelectrolytes and either anionic or cationic surfactants according to the charge of the polypeptide. Complexes of poly(α-amino acid)s such as poly(α,L-glutamic acid) and poly(α,L-lysine) with alkyltrimethylammonium bromides or sodium alkyl sulfonates, respectively, were investigated by Ponomarenko et al.[7] In these complexes, the main chain is arranged in the α-helical conformation typical of poly(α-amino acid)s. More recently, new polypeptidic complexes have been prepared from microbial poly(γ-glutamic acid) with either racemic or enantiomeric enriched composition[8] and found to display a very similar behavior to that described for complexes made of conventional poly(α-amino acid)s. In this case, however, the poly(γ-peptide) seems to be arranged in a more or less extended conformation, likely due to the different density and distribution of charges along the polypeptidic chain.[9] Nevertheless, polypeptide−surfactant complexes are invariably organized in biphasic structures with the polypeptide chains arranged in layers that are regularly spaced by intercalating surfactant molecules. These assemblies are very similar to those adopted by their covalent analogous comblike alkyl esters of poly(α-glutamic acid)[10] and poly(γ-glutamic acid).[11]

In this paper, we wish to report on the complexes synthesized from poly(β,L-malic acid) and alkyltrimethylammonium bromides with the alkyl group being linear and containing even numbers of carbon atoms from 14 up to 22. These complexes will be referred henceforth as *n*ATMA·PMLA. Poly(β,L-malic acid) (PMLA) is an assimilable and readily biodegradable polyester that can be prepared either by chemical synthesis or by biosynthesis from myxomycetes and different species of fungi.[12] The possibility that poly(β,L-malic acid) may form stable complexes with oppositely charged low molecular weight compounds opens interesting opportunities for the potential

* Corresponding author. E-mail: sebastian.munoz@upc.es.
† Universitat Politècnica de Catalunya ETSEIB.
‡ Institut für Biophysik und Physikalische Biochemie der Universität.

10.1021/bm050490t CCC: $33.50
Published on Web 11/22/2005

applications of this natural biopolyester. This work should be envisaged therefore as the first step of research addressed to explore the utility of amphiphilic PMLA-based nanostructures in biomedicine, specifically as a biodegradable drug encapsulating system. The evaluation of the degradability and drug delivery properties of these *n*ATMA·PMLA complexes is a matter of work currently under course in our laboratory.

Experimental Section

Materials. PMLA of microbial origin was used in this work. It was obtained by cultivation of *Physarum polycephalum*. The polyacid was NMR pure and it had a $M_w = 26\,000$ Da and $M_w/M_n = 1.25$. Linear alkyltrimethylammonium surfactants of general formula $RN^+(CH_3)_3{\cdot}Br^-$ with R = $C_{12}H_{25}$ (dodecyl), $C_{14}H_{29}$ (meristyl), $C_{16}H_{33}$ (cetyl), and $C_{18}H_{37}$ (stearyl) were purchased from Aldrich or Merck and used as received. Those with R = $C_{20}H_{41}$ (eicosyl) and $C_{22}H_{45}$ (docosyl) were synthesized specifically for this work following the amine quaternization method described in the literature for the preparation of certain alkylaromatic amines.[13] Organic solvents were of analytical grade and used without further purification. Water used in the preparation of the complexes was distilled and deionized in a "Milli-Q" water purification system.

Conditions for Growth and PMLA Production. Microplasmodia of *P. polycephalum* (strain M3CVII, ATCC 204388) were cultivated in flasks and preserved in the form of spherules as described by Daniel and Baldwin (1964).[14] A vegetative seed culture was prepared from spherules in 100 mL of basal medium on a rotary shaker (60 rpm, pH 4.5, 24 °C, in the dark). After 5 days, the microplasmodia were subcultivated 2 ± 3 times by transfer to 100 mL of basal medium at pH 4.5 in 500 mL Erlenmeyer flasks (2 days at 24 °C), and then microplasmodia were washed and inoculated in a 20 L bioreactor. The fermentation lasted for 4−5 days at 24 °C, 150 rpm, and an air flow of 10 vvm. The culture medium contained 33 g L^{-1} D-glucose, 10 g L^{-1} bactotryptone, 3.5 g L^{-1} citric acid monohydrate, 2.0 g L^{-1} KH_2PO_4, 1.0 g L^{-1} $CaCl_2{\cdot}2H_2O$, 0.6 g L^{-1} $MgSO_4{\cdot}7H_2O$, 0.085 g L^{-1} $MnCl_2{\cdot}4H_2O$, 0.085 g L^{-1} $FeSO_4{\cdot}7H_2O$, 0.035 g L^{-1} $ZnSO_4{\cdot}7H_2O$, 0.0025 g L^{-1} hematin, and 40% w/v $CaCO_3$. Hematin (0.25 g L^{-1}in 0.25 M NaOH) and $CaCO_3$ solutions were autoclaved separately and added to the cooled medium. The pH of the medium was adjusted to 4.5 before sterilization with NaOH 5M.

Isolation and Purification of PMLA from Culture. The method used is a modification of the method reported by Holler (1997).[15] The pH of the culture broth was adjusted to 7.5, and cells were removed by centrifugation at 800*g* for 10 min. The supernatant was diluted with 0.05 M TRIS−HCl, buffer pH 7.5 and poured into a DEAE-cellulose. The fractions were collected by stepwise elution with NaCl-TRIS buffer pH 7.5. The polymer-containing fractions were adjusted to 0.1 M $CaCl_2$, 80% ethanol, and left for 12 h at −20 °C for polymer precipitation. The polymer was pelletized by centrifugation and washed several times with 80% ethanol. After desalting over Sephadex G-25, it was lyophilized. The pure calcium salt was changed to the acid form by passage over Amberlite 120 (H^+-form) and lyophilized after neutralization of the solution. For quantification, PMLA was hydrolyzed in 1 M sulfuric acid, and L-malate was assayed by the method of Bergmeyer (1974).[16]

Gel permeation chromatography (GPC) was performed with a Waters equipment provided with refraction-index and light-scattering detectors. Chromatography was carried out in phosphate buffer pH 7.0, and chromatograms were calibrated against poly(ethylene oxide) (PEO). The specific refractive index increment (d*n*/d*c*) was estimated from an injected mass, at 25 °C in an Optilab refractometer from Wyatt, resulting in a value of 0.140 mL g^{-1}.

Synthesis of Complexes. Complexes of poly(*β*,L-malic acid) were prepared following the methodology described by Ponomarenko et al.[7] for the synthesis of complexes of the same type of surfactants with poly(α,L-glutamic acid) and used by us for the complexation of poly(*γ*-glutamic acid).[8] In brief, 50 mL of an aqueous 0.01 M solution of the surfactant of choice was added, under stirring, to the same volume of a 0.01 M of PMLA solution in phosphate buffer pH 7.0 to be sure that the PMLA is dissociated ($pK_a = 3.45$), and the mixture was left to rest at room temperature. A white precipitate appeared in a few minutes, which was isolated by centrifugation, washed several times with water, and dried under vacuum at 30 °C for at least 48 h. Complexes with *n* = 18, 20, and 22 were obtained by mixing the surfactant and PMLA solutions at 40 °C.

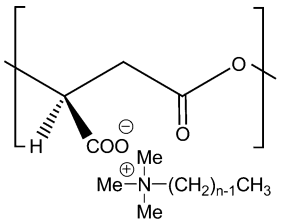

*n*ATMA·PMLA (*n* = 14,16,18, 20, 22)

Figure 1. Chemical formula of complexes studied in this work.

Measurements. FTIR spectra were recorded on a Perkin-Elmer FT-2000 instrument from films prepared by casting from chloroform solution. ^1H and ^{13}C NMR spectra were recorded on a Bruker AMX-300 NMR instrument provided with a CP-MAS accessory for the analysis of solids. Analysis in solution of the complexes was carried out with samples dissolved in $CDCl_3$ and using TMS as reference, and the analysis of poly(*β*,L-malic acid) in deuterated DMSO. Solid state ^{13}C CP-MAS NMR spectra were recorded at 75.5 MHz in the temperature range of 20−90 °C from 200 mg of powder samples that were spun at 3.9−4.0 kHz in a cylindrical ceramic rotor. All of the spectra were acquired with contact and repetition times of 2 ms and 5 s, respectively, and 1024 transients were accumulated. The spectral width was 31.2 kHz, and the number of data points was 4K. Chemical shifts were externally calibrated against the higher field peak of adamantane appearing at 29.5 ppm relative to TMS. Calorimetric measurements were performed with a Perkin-Elmer Pyris DSC instrument calibrated with indium. Sample weights of about 2−5 mg were used at heating and cooling rates of 10 °C min^{-1} and under a nitrogen atmosphere. Thermogravimetric analyses were performed under an inert atmosphere with a Perkin-Elmer TGA6 thermobalance at a heating rate of 10 °C min^{-1}. Optical microscopy was carried out in a Olympus BX51 polarizing microscope equipped with a digital camera system and a Linkam THM5600 hot stage. Filmy samples of *n*ATMA·PMLA of complexes were prepared from 1% (w/v) chloroform solutions, which were left to evaporate slowly between two microscope cover slides.

X-ray diffractograms were obtained in a diffractometer with geometry Debye−Scherrer INEL CPS-120, detector sensible to position 120°, 4096 measure channels and acquisition time of 4200s. The Cu Kα radiation of wavelength 0.1541 nm was used in all cases.

Results and Discussion

Synthesis and Characterization. The preparation of the *n*ATMA·PMLA complexes, with the chemical structure depicted in Figure 1, was carried out by common precipitation of equimolar amounts of the two components (PMLA and *n*ATMA bromide salts) from aqueous solution, which is the usual procedure described in the literature for the synthesis of polyelectrolyte-surfactant complexes. The temperature was chosen as close as possible to room temperature provided that a complete solubility of the surfactant in water was attained, and the pH was adjusted at 7.0, at which more than 99% of the carboxylate groups of PMLA are in the ionized state. The complexes were recovered as white finely divided powders that could be comfortably handled. By this means, complexes for *n* = 14, 16, 18, 20, and 22 were obtained in yields ranging between 77 and 99% indicating that complexation occurred

Table 1. Poly (β,L-malic acid)−Surfactant Complexes *n*ATMA·PMLA: Synthesis Results

					elemental analysis[c]			
R	complex	T[a] (°C)	yield (%)	composition[b]	C (%)	H (%)	N (%)	ρ (g mL^{-1})
$-C_{14}H_{29}$	14ATMA·PMLA	25	78	1.0	60.52 (61.90)	10.47 (10.14)	3.37 (3.40)	1.00
$-C_{16}H_{33}$	16ATMA·PMLA	25	88	1.1	62.35 (62.81)	10.70 (11.10)	3.23 (3.48)	1.00
$-C_{18}H_{37}$	18ATMA·PMLA	40	93	1.0	64.74 (65.91)	11.12 (11.71)	2.86 (3.10)	1.01
$-C_{20}H_{41}$	20ATMA·PMLA	40	99	1.1	66.25 (66.91)	11.37 (11.00)	2.73 (2.92)	1.01
$-C_{22}H_{45}$	22ATMA·PMLA	40	91	1.3	66.03 (65.02)	11.81 (13.3)	2.71 (3.33)	1.02

[a] Complexation temperature. [b] Molar ratio of *n*ATMA to PMLA in the complex as estimated by ^{1}H NMR. [c] In brackets, values calculated for the observed compositions and assuming 2 molecules of absorbed water per repeating unit.

Table 2. ^{13}C and ^{1}H NMR Chemical Shifts[a] (δ, ppm) of *n*ATMA·PMLA Complexes and Their Components

	main chain					side chain								
	COO	α-CH_2		β-CH		COO	NCH_3		NCH_2		CH_3		$(CH_2)_{2-(n-1)}$	
complex	^{13}C	^{13}C	^{1}H	^{13}C	^{1}H	^{13}C	^{1}H	^{13}C	^{1}H	^{13}C	^{1}H	^{13}C	^{1}H	^{13}C
14ATMA·PMLA	171.4	37.1	3.0; 2.7	71.3	5.2	172.9	3.2	53.1	3.5	66.7	0.9	14.1	1.3−2.3	22.6−31.9
14ATMA·Br							3.5	53.3	3.6	66.8	0.9	14.1	1.3−1.8	22.6−31.9
16ATMA·PMLA	171.4	37.2	3.0; 2.8	71.3	5.2	172.5	3.2	53.1	3.5	66.7	0.9	14.1	1.3−2.3	22.6−31.9
16ATMA·Br							3.5	53.4	3.6	66.9	0.9	14.1	1.3−1.8	22.7−31.9
18ATMA·PMLA	170.7	37.2	3.0; 2.8	71.7	5.2	173.0	3.2	53.1	3.5	66.7	0.9	14.1	1.3−2.3	22.6−31.9
18ATMA·Br							3.5	53.3	3.6	66.9	0.9	14.1	1.3−1.8	22.7−31.9
20ATMA·PMLA	170.7	37.1	3.0; 2.7	71.8	5.2	172.5	3.2	53.1	3.5	66.7	0.9	14.1	1.3−2.3	22.6−31.9
20ATMA·Br							3.5	53.4	3.6	66.8	0.9	14.1	1.3−1.8	22.7−31.9
22ATMA·PMLA	170.8	37.3	3.0; 2.7	72.0	5.2	172.4	3.2	53.1	3.5	66.7	0.9	14.1	1.3−2.3	22.6−31.9
22ATMA·Br							3.5	53.3	3.6	66.8	0.9	14.1	1.3−1.8	22.6−31.9
H−PMLA [b]	168.2	35.1	2.9	68.3	5.3	169.4								

[a] Spectra recorded in $CDCl_3$. [b] Spectra recorded in deuterated DMSO.

Table 3. Thermal Behavior[a] and X-ray Diffraction Spacings[b] of *n*ATMA·PMLA.

	TGA and DSC								X-ray diffraction spacings	
complex	T_d (°C)	T_m1 (°C)	T_m2 (°C)	T_c (°C)	ΔH_m2 (kcal mol^{-1})	%CH_2 cryst	T_i (°C)	ΔH_i (kcal mol^{-1})	side chain (nm)	L_0 (nm)
14ATMA·PMLA	219	n.o.	n.o.	n.o	n.o.	0	94	1.5	0.45br	3.2s; 1.6 w
16ATMA·PMLA	224	29	30	16	1.2	8	94	1.6	0.415m; 0.45br	3.6s; 1.8w
18ATMA·PMLA	232	50	48	35	3.4	18	95	1.7	0.415m	3.8s; 1.9w
20ATMA·PMLA	234	60	60	50	5.4	27	98	1.9	0.415m	4.0s; 2.0w
22ATMA·PMLA	236	72	71	66	6.8	31	104	2.2	0.415m	4.3s; 2.15w

[a] T_d: Onset decomposition temperature measured at 5% of loss of initial weight; T_m: melting temperature at first heating (1) and second heating (2); T_c: crystallization temperature; T_i: isotropization temperature. ΔH_m: enthalpy of melting; ΔH_i: enthalpy of isotropization. [b] Spacings measured from powdered samples; visual intensities denoted as s, strong; m, medium; w, weak; br, broad.

extensively in all cases. Attempts to obtain the complex 12ATMA·PMLA failed because the precipitated product redissolved during the isolation procedure. Results obtained for the five complexes examined in this study are compared in Table 1.

The constitution of the complexes was first ascertained by FTIR. A comparison of the spectra of PMLA and *n*ATMA·PMLA shows that the characteristic carboxylic group vibrations appearing for PMLA at 3565 and 1745 cm^{-1} (H−O and C═O stretching, respectively) are absent in the spectra of the complexes. In contrast, a new band at 1607 cm^{-1}, which is characteristic of the ionized carboxylate group, is common to the spectra of all complexes. On the other hand, none of the stretching absorptions arising from the main chain ester groups (C═O and C−O−C) seemed to be significantly affected in the complexes. NMR spectroscopy afforded definite proof of the constitution of *n*ATMA·PMLA compounds. Illustrative spectra are shown in Figure 2 for the case of 20ATMA·PMLA and both ^{1}H and ^{13}C NMR data recorded for the complexes and for the respective surfactants in the same solvent are compared in Table 2. Both ^{1}H and ^{13}C signals arising from N−CH_3 and N−CH_2 appear invariably displaced to higher field in the complexes indicating the smaller inductive charge effect exerted by the carboxylate group when compared to the bromide ion. Comparison of complexes spectra to the spectrum of PMLA registered in DMSO afforded also eloquent differences in the chemical shifts of both protons and carbon of the main chain. The main chain ^{13}C signals of *n*ATMA·PMLA appear moved to lower field whereas the ^{1}H signals broaden as a consequence of the restriction in mobility that is imposed by the presence of the ionic groups. These differences are not totally conclusive since it cannot be discarded to be caused in part by solvent effects.

The spectra produced by the alkyl side chain are practically undistinguishable for all of the complexes except in the area of the signals arising from the inner methylenes, which increases proportionally to the value of *n*, as it should be anticipated. Comparison of the peak areas measured for main chain and side chain protons signals observed in the ^{1}H NMR spectra afforded an accurate estimation of the ionic composition of the complexes. These results are shown in Table 1 where it is seen that the cation-to-anion ratio appears to be 1 or near to 1, the only significant deviation being found for 22ATMA·PMLA, which contains around 30% of surfactant in excess. Several attempts

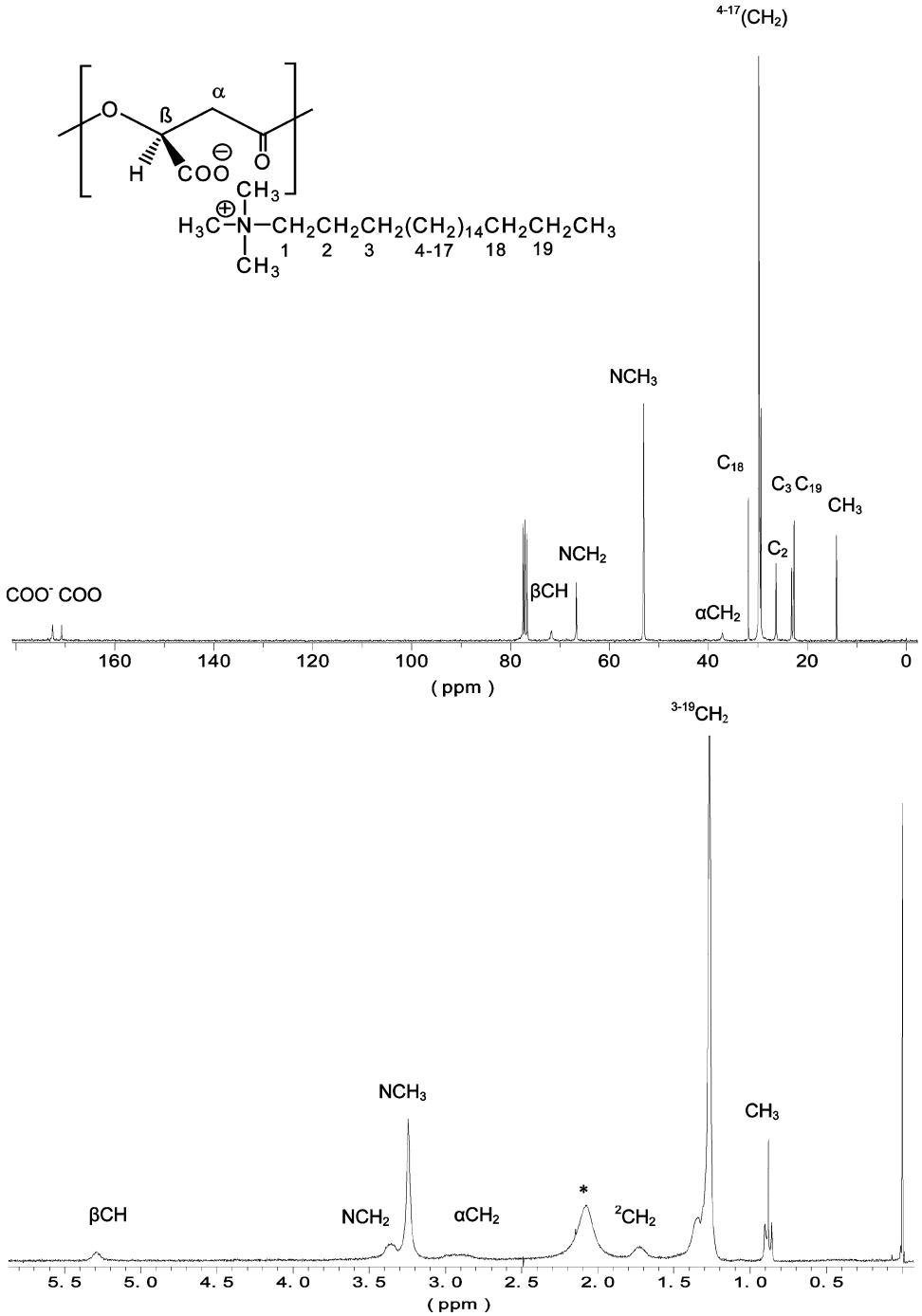

Figure 2. ^{1}H (bottom) and ^{13}C (top) NMR spectra of 20ATMA·PMLA recorded at 25 °C. (∗) Peak of water.

made to remove the exceeding surfactant by exhaustive washing were unsuccessful. Combustion analyses were in agreement with calculated elemental compositions provided that a certain amount of water ranging between 6 and 9% w/w is assumed to be present in the compound. The presence of this water is detected in the ^{1}H NMR spectra as a peak at around 2.1 ppm. Such water must be firmly attached to the complex since it could not be removed by drying under high vacuum for several days. Analyses of residual bromide were in the range expected for the compositions determined by NMR. Densities of complexes were found to be around unity, a value significantly lower than those of the pure components, which are about 1.3−1.4. Although this decreasing in density is what should be expected from the removal of the bromide ions, it indicates also that the packing of the structure must be more loosen in the complexes.

The solubility behavior displayed by *n*ATMA·PMLA complexes is more limited than that observed for complexes of poly(amino acid)s and oppositely charged surfactants,[7,8] being soluble only in chloroform and in low polar protic solvents such as methanol and ethanol. In highly polar solvents, the polyelectrolyte−surfactant complexes are likely to be partially dissociated, whereas in nonpolar solvents, they should be expected to remain tightly associated. An interesting feature worth mentioning is that *n*ATMA·PMLA are readily soluble in chloroform, whereas they cannot be dissolved by water, which is exactly the opposite behavior showed by Na·PMLA and *n*ATMA·Br.

The thermal stability of *n*ATMA·PMLA complexes was first examined by thermogravimetry in order to define the usable temperature range and to ensure the reliability of the calorimetric

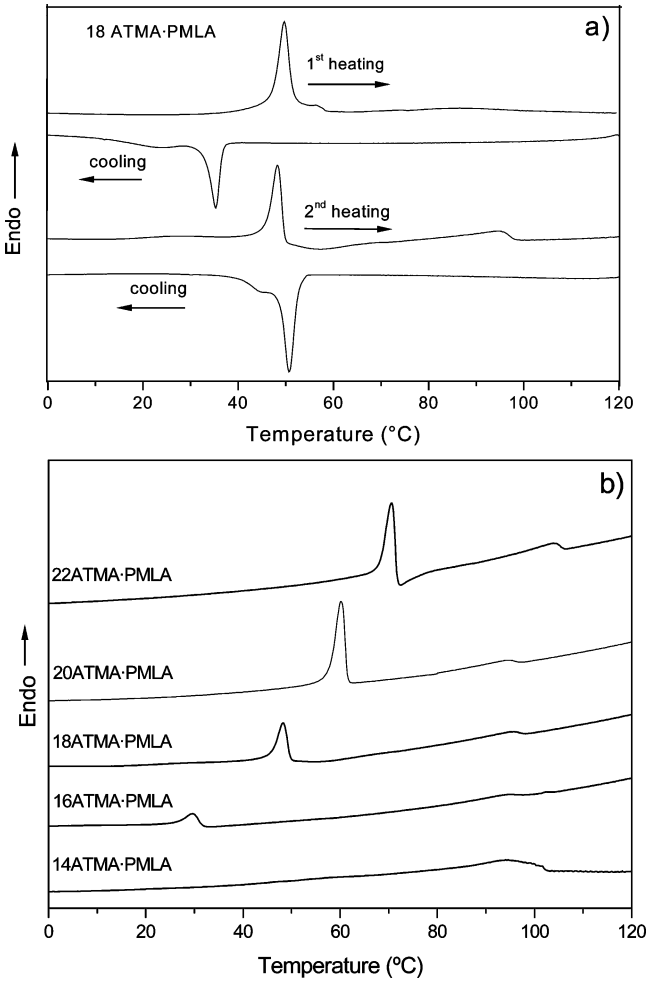

Figure 3. DSC traces of *n*ATMA·PMLA complexes. (a) First heating, cooling, and reheating of 18ATMA·PMLA. (b) Second heating traces compared for the whole series.

experiments that were then carried out. The onset decomposition temperatures for all of the complexes are given in Table 3. They were found to be quite stable below 200 °C to decompose through a three-step decomposition process with maxima decomposition rates taking place near 250 °C. It can be said that the thermal stability of these complexes is rather lower than that of polymeric ionic complexes made of polypeptides indicating that it is the polyester chain which determines the first decomposition step. An analytical study is under course to elucidate in detail the molecular mechanism underlying the thermal decomposition of *n*ATMA·PMLA complexes.

Solid-State Structure. DSC analysis revealed significant differences in the thermal behavior of *n*ATMA·PMLA complexes according to the value of *n*. The thermograms obtained from 16, 18, 20, and 22ATMA·PMLA exhibited well-defined melting peaks at increasing temperatures from 30 up to 70 °C, which could be fairly reproduced after cooling and subsequent reheating. This peak was not observed in the thermograms registered for the 14ATMA·PMLA complex indicating absence of crystallinity in this complex. It should be noted that DSC of H−PMLA recovered from aqueous solutions does not show any thermal transition before degradation[17] and that melting of alkyltrimethylammonium bromides takes place within the range of 100−150 °C. By analogy to thermal data reported for analogous *n*ATMA·PGGA complexes[8] as well as for comblike poly(glutamate)s,[10,11] the endothermic peak is interpreted as being due to the fusion of the polymethylene side chain, which

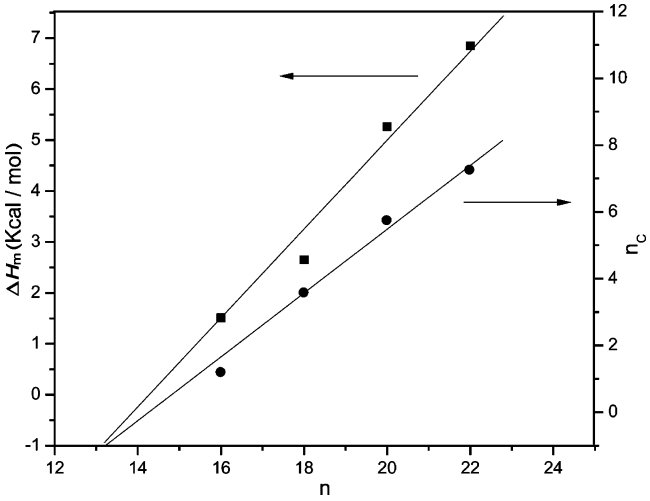

Figure 4. Melting enthalpy (ΔH_m) and number of crystallized methylene units (n_c) as a function of *n*.

was able to crystallize for a number of carbon atoms higher than 14. This thermal behavior is also similar to that previously reported for long chain *n*-alkylammonium polyacrylates.[18] The complete DSC sequence (first heating, cooling and reheating) obtained from 18ATMA·PMLA as well as the reheating traces for the whole *n*ATMA·PMLA series are shown in Figure 3. Melting temperatures and enthalpies are listed in Table 3.

It is well-known that crystallization of the alkyl side chain of comblike polymers is by no means complete, the fraction of crystallized methylenes being estimated from the melting enthalpy measured by DSC. A linear correlation between ΔH_m and *n* is usually observed for all comblike polymers with attached flexible polymethylene side groups, which is well represented by eq 1[19]

$$\Delta H_m = \Delta H_m^\circ + nk \qquad (1)$$

where ΔH_m° and *k* are constants reflecting the contribution of the side chain end group and each added methylene unit to the global melting enthalpy, respectively. Jordan et al.[20] reported that the number of crystallized CH_2 units in the side chain may be calculated from eq 1 simplified as $\Delta H_m = n_c k$. Although this approach only allows a rough evaluation of n_c, it has been repeatedly used with satisfactory results for a wide variety of comblike polymers.[8−11]

As it can be seen in Table 3, ΔH_m of *n*ATMA·PMLA increases steadily with the length of the alkyl side chain as it does therefore the number of methylenes taking part of crystallites located in the paraffinic phase. The plots of melting enthalpy and crystallized methylenes number against *n* are depicted in Figure 4 revealing the linear dependence that exists in both cases. The value of *k*, graphically evaluated from the plot of Figure 4, is 0.96 kcal/mol of CH_2. This value is quite close to the value of 1.0 kcal mol^{-1} of CH_2 that is reported for the solid-to-liquid melting transition taking place in the homologous series of alkanes and in polyethylene.[21] The average number of crystallized methylenes, n_c, is determined to vary from 1.2 for 16ATMA·PMLA to 7.3 for 22ATMA·PMLA, with a nearly fixed amount of about fourteen methylene units remaining in a disordered state. The fraction of the polymethylene segment participating in the crystallization varies therefore from 8 to 31%, whereas no crystallization is observed for 14ATMA·PMLA.

A comparison of these DSC results with those previously obtained by us with other poly(carboxylic acid)−ATMA sur-

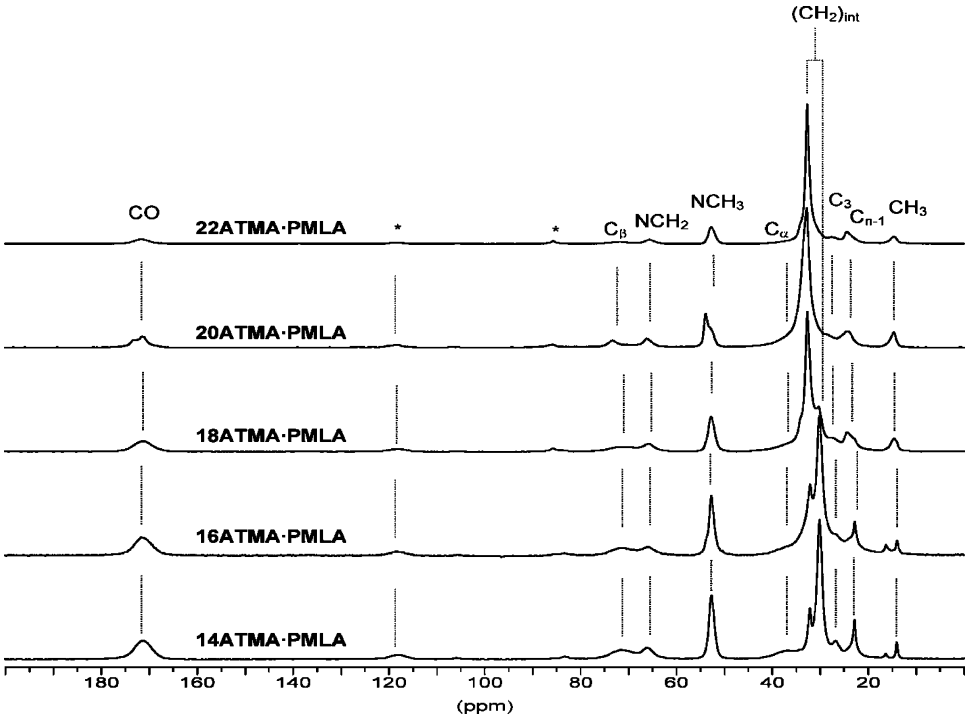

Figure 5. ^{13}C CP-MAS NMR spectra of *n*ATMA·PMLA complexes recorded at 20 °C. Asterisk (∗) indicates spinning side bands.

factant complexes[8] reveals that, for a given value of *n*, the crystallization of the alkyl side chain takes place in a similar extension and that the melting temperature of the crystallized material is very similar. Thünemann and General[22] studied in detail the crystallization and melting transition in poly(ethylene imine) *n*-alkyl carboxylate complexes, a system in which the locations of the two counterions are reversed. They found lamellar structures with T_m increasing from −2 up to 83 °C and the fraction of crystallized methylene units oscillating between 1.6 and 70% for carboxylic acids with a number of carbon atoms ranging from 12 to 26. Apparently, crystallization of the polymethylene side chain is relatively favored in this system, which could be due to the less influence exerted by the secondary amine group in comparison to the alkyltrimethylammonium group.

Additional information on the structure of the paraffinic phase was afforded by ^{13}C CP-MAS NMR analysis. The spectra of solid *n*ATMA·PMLA complexes recorded at 20 °C are compared in Figure 5. No significant differences in the signals arising from the main chain were found indicating that, as it should be expected, polymalate must be arranged in the same conformation in all of the complexes. Conversely, the signals assigned to the carbon atoms contained in the surfactant counterpart appeared to be sensitive to the value of *n* confirming the occurrence of structural differences according to the length of the alkyl group. Specifically, the intense signal arising from the interior methylenes, which is displayed as a single peak at ∼33 ppm for 22ATMA·PMLA and 20ATMA·PMLA, appears split for the other lower members of the series, the new peak at ∼30 ppm increasing in relative intensity as the value of *n* decreases. According to previous studies carried out by us,[11,23] the lower field peak is ascribed to crystallized methylenes in trans conformation, whereas the higher field one arises from methylenes that are in a fast trans−gauche equilibrium. The differences observed reveal therefore that the all-trans arrangement inherent to the full-extended conformation of the crystallized polymethylene segment is common to the higher members of the series to practically disappear for 16ATMA·PMLA and 14ATMA·PMLA. In these last two cases, the alkyl side chains mostly remain in the molten state at the temperature of the observation with torsion angles in a narrow span around 180°.

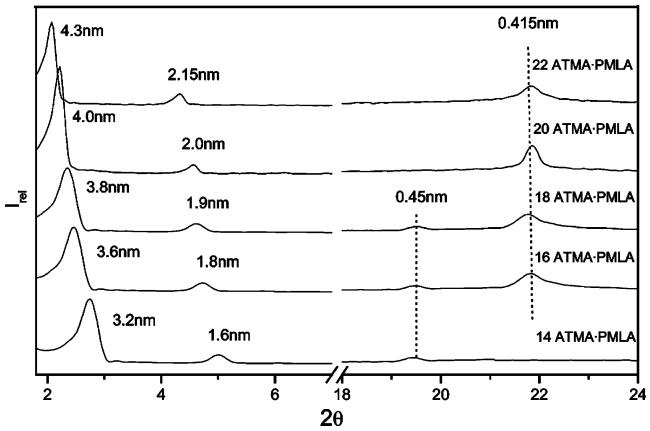

Figure 6. Diffractograms of *n*ATMA·PMLA complexes at room temperature.

Powdered samples of *n*ATMA·PMLA complexes were subjected to X-ray diffraction over a wide span of angles in order to record simultaneously structural data on both nanometric and subnanometric scale. Discrete diffraction peaks revealing the existence of an ordered structure were observed in the scattering curves of complexes with $n \geq 16$, which is in full agreement with the DSC results described above. The scattering profiles recorded for these members are compared in Figure 6 and the Bragg spacings observed for the whole series are listed in Table 3. According to antecedents, the sharp diffraction peak with a spacing of 0.415 nm appearing within the wide-angle region is associated to the scattering produced by the crystallites made of partially crystallized alkyl side chains, the spacing being interpreted as the 100 interplanar distance of a hexagonal lattice of $a = 0.48$ nm. Such scattering is clearly different from that observed for crystallized alkyltrimethylammonium bromide salts, which consists of two reflections at 0.39

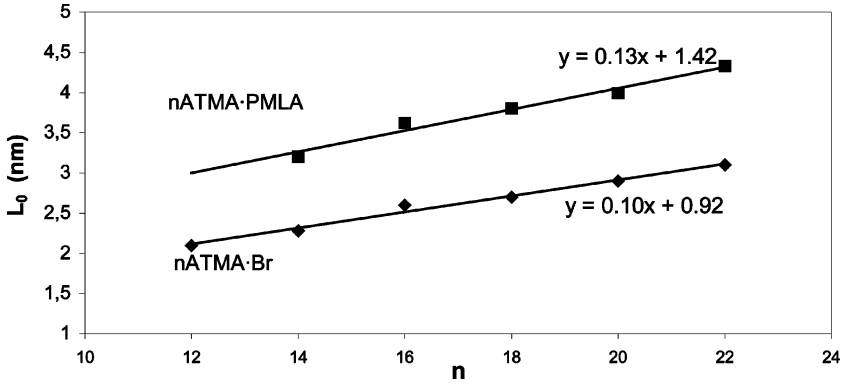

Figure 7. Interlayer distance of the biphasic structure in *n*ATMA·PMLA complexes and long spacings observed for the corresponding surfactant salts plotted against the number of carbon atoms in the alkyl side chain.

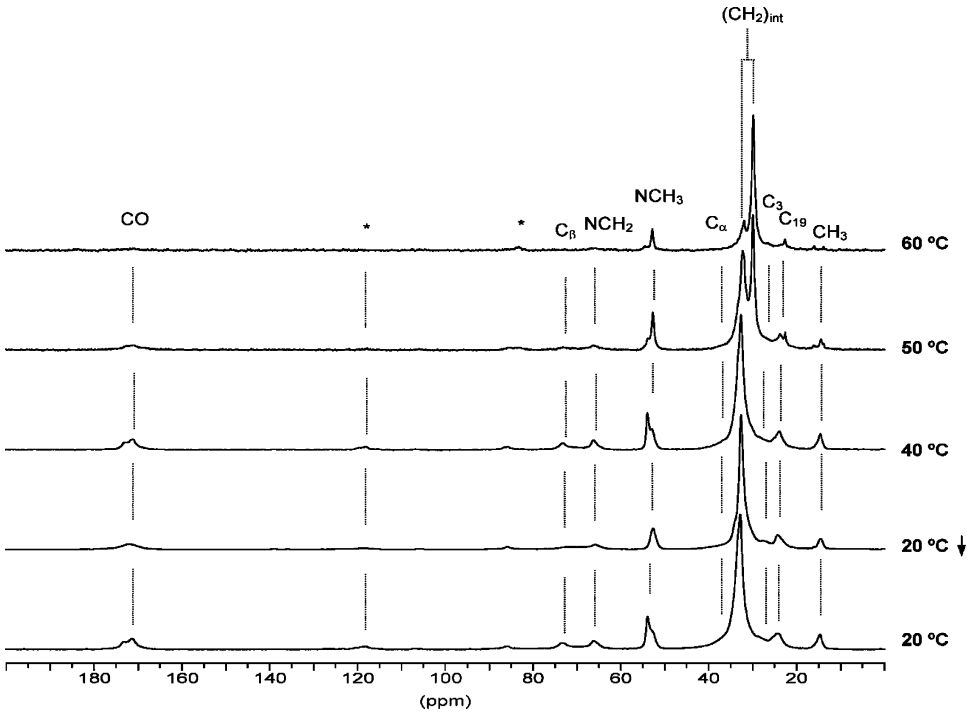

Figure 8. ^{13}C CP-MAS NMR spectra of 20ATMA·PMLA at the indicated temperatures. Asterisk (*) indicates spinning side bands.

and 0.35 nm characteristic of a lattice with the alkyl chains packed in a monoclinic array. It should be noted however that the scattering produced by 14ATMA·PMLA in this region consists of a broad peak centered at 0.45 nm. This scattering is interpreted as arising from the average interchain distance of the paraffinic phase with chains longitudinally aligned in a partially disordered state, which is fully coherent with the incapacity of this complex to crystallize as evidenced by DSC. Both peaks, at 0.415 and 0.45 nm, were present in the pattern recorded from 16ATMA·PMLA according to the intermediate nature of this complex.

In the small angle region, all the complexes showed discrete diffraction scattering corresponding to the first and second order of a main spacing that increases steadily from 3.20 nm for 14ATMA·PMLA up to 4.30 nm for 22ATMA·PMLA. According to what is known for other comblike ionic complexes made of anionic polyelectrolytes and cationic surfactants, such spacing, L_0, is associated to the periodicity of a layered biphasic arrangement in which the paraffinic phase made of alkyl side chains alternates with the phase made of polymalate main chains. Plotting of L_0 against the number of carbon atoms contained in the alkyl group of the surfactant (Figure 7) resulted in a straight line with slope 0.130 nm and crossing the ordinates axis at 1.42 nm. It is inferred from these data that the alkyl side chains must be oriented normal or very near to the normal to the layer planes and that they are extensively interdigitated. Furthermore, the fact that the long spacings measured for 14ATMA·PMLA and 16ATMA·PMLA fit well in the straight line of the series, in spite of the fact that the side chain in these complexes is in the noncrystallized state, indicates that the conformation of the alkyl group must be nearly extended in these compounds.

The structural changes encompassing the melting-crystallization of the alkyl side chain in the *n*ATMA·PMLA complex were followed by ^{13}C CP-MAS NMR and X-ray diffraction. The solid state ^{13}C NMR spectra recorded for 20ATMA·PMLA at increasing temperatures from 20 up to 60 °C are shown in Figure 8. Comparison of these spectra reveals differences among them similar to those noticed in Figure 5, but in this case as a function of temperature. Below T_m, which is 60 °C in this complex, the position and intensity of the signals arising from the inner methylenes of the alkyl side chain indicate that it is in the all-trans conformation characteristic of the crystallized state whereas a mixed population of gauche and trans arrangements is present above such temperature. The diffractograms of 18ATMA·PMLA registered at increasing temperatures from 20 up to 120 °C are compared in Figure 9. Upon heating at 60 °C, the initially

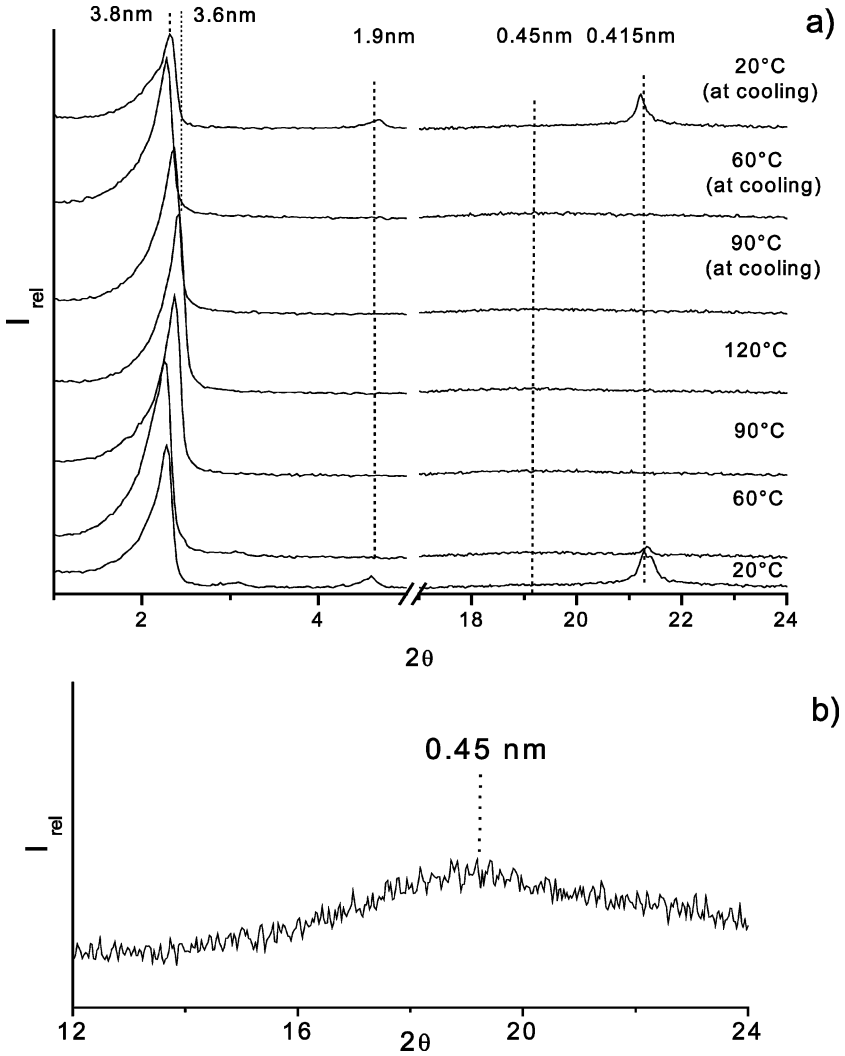

Figure 9. (a) Thermodiffractograms of 18ATMA·PMLA at the indicated temperatures. (b) Wide angle region of the diffractogram of 18ATMA·PMLA recorded at 120 °C enlarged along the I_{rel} axis to illustrate the presence of the 0.45 scattering in the heated complex.

present 0.415 nm diffraction peak moved to 0.45 nm and broadened. This change reflects the occurrence of a melting process of the polymethylene crystallites in which the molten chains retain their lattice positions. Additional changes took place however in the region of low angles ($2\theta < 5°$) indicative of that dimensions of the supramolecular structure were also affected by heating. Whereas no significant dimensional variations happened below T_m, a slight but well-defined contraction of about 0.2 nm took place upon heating through the 60−120 °C range. It is worth mentioning that the conformational changes observed for the alkyl chains taking place in these complexes upon heating are similar to those reported for other comblike systems studied previously by us, as long alkyl polyaspartates[23] and polyglutamates[11] and *n*ATMA·PGGA[8] complexes. Conversely, a different behavior has been reported for the case of surfactant−polyacrylate complexes studied by Tsiourvas et al.,[18] who described for the high temperature phase a double layer arrangement with alkyl chains in a largely disordered conformation. Furthermore, a large hysteresis for the paraffinic melting-crystallization process, which is consistent with the occurrence of an extensive molecular rearrangement, was observed in these systems.

According to the biphasic model, the ordinate value resulting for $n = 0$ in the L_0-n plot (Figure 7) would correspond to the lateral size of the polymalate chain including the trimethylammonium counterpart. A parallel straight line displaced down along the ordinates by about 1 nm was obtained for the *n*ATMA·Br salts in agreement to what should be expected from the smaller space occupied by the bromide anions as compared to the anionic polymalate chain. Very preliminary studies have put forward that the un-ionized polymalic acid in solution is a random coil, whereas a nearly extended conformation seems to be preferred when the polyester is in the ionized form. Since nothing relative to the structure of PMLA in the solid state has been published to date and no data specific to the main chain phase could be obtained along this study, the arrangement adopted by the polymalate chain in the biphasic structure of *n*ATMA·PMLA complexes cannot be outlined. Nevertheless, the structural features displayed by the complexes and their regular dependence on their molecular constitution suggest that the main chain must be regularly arranged, probably in extended or nearly extended conformation. In this regard, it is noteworthy that the distance between the carboxylate groups along the fully extended polymalate chain is about 0.48 nm, which coincides with the interchain spacing in the crystallites made of alkyl side chains.

The lamellar thickness range ($L_0 = 3.60-4.30$ nm) found for *n*ATMA·PMLA with crystallized alkyl side chains ($n = 16-22$), is of the same magnitude that for the same set of complexes made of poly(γ-glutamic acid) and alkyltrimethylammonium surfactants.[8] In this system, the ionic pair is of the same nature than in *n*ATMA·PMLA and it is also directly attached to the

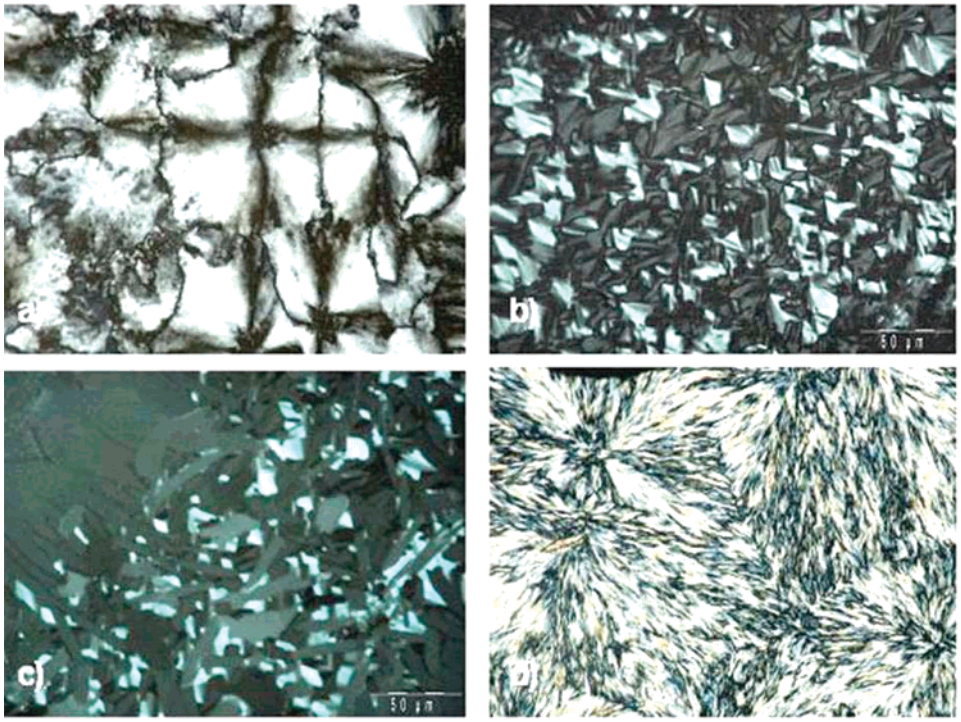

Figure 10. Polarizing optical micrographs of 18ATMA·PMLA. (a) 20 °C; Film grown from the melt (first heating); (b) 85 °C; Smectic LC texture displayed between the melting point and the isotropic temperature; (c) 85 °C; Smectic LC texture reappeared upon cooling from the isotropic phase; (d) 20 °C; Spherulitic texture reappeared upon cooling below T_m (second heating).

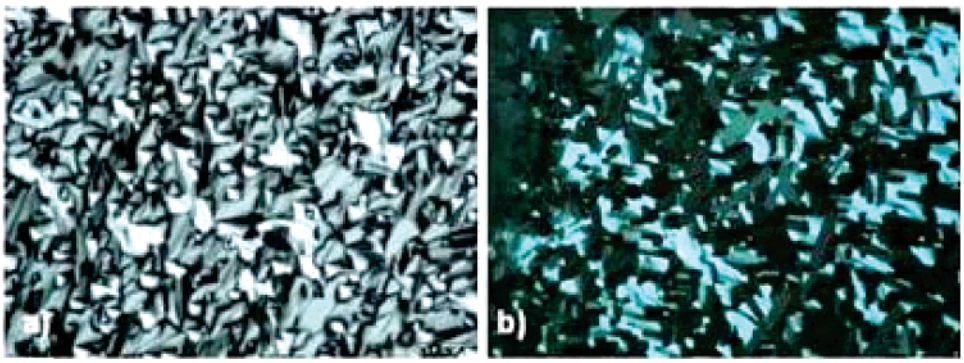

Figure 11. Polarizing optical micrographs of 14ATMA·PMLA. (a) Texture below the isotropic temperature. (b) Texture recovered upon cooling to room temperature the isotropicized sample.

polymer backbone. The polymer main chain is assumed to be in an extended or almost extended conformation in both cases. Conversely, the lamellar thickness in the complexes made from poly(α-glutamic acid)[7] was reported to be significantly higher. In these complexes, not only is the ionic pair separated from the main chain by an ethylene unit but poly(α-peptide) is in the helical conformation. Both are good reasons to explain adequately the observed differences. On the other hand, comparison with the poly(ethylene imine)−carboxylate complexes provides an additional interesting perspective. For similar alkyl chain lengths, the lamellar thickness reported for this system is about 3−5 nm shorter than in *n*ATMA·PMLA complexes revealing a higher packing of the structure. Furthermore, the lamellar thickness increases only ∼0.08 nm per methylene unit, which is in agreement with an array of side chains tilted with respect to the lamellar plane with an average angle of approximately 40°.

Liquid Crystal Behavior. The occurrence of a stiff molecular structure, as it would result from the repulsive interaction between adjacent ionic pairs along the alkyltrimethylammonium polymalate chain, is expected to display liquid crystal behavior at temperatures above the melting of the paraffinic crystal phase. A close inspection of the DSC traces shown in Figure 3b reveals on the second heating traces of all of the *n*ATMA·PMLA complexes the presence of a weak endothermic peak of reversible nature at temperatures near to 100 °C (T_i). Such a weak heat exchange should not be related to a melting process but rather to a structural transition associated to the existence of a mesophase. The existence of mesophases with either smectic or nematic structure is almost a characteristic of comblike polymers made of stiff main chains and flexible side chains.[2] The analysis by polarizing optical microscopy revealed the crystalline nature of the complexes at temperatures below T_m and afforded evidences on the occurrence of a liquid crystal phase between T_m and T_i. The sequence of events taking place when 18ATMA·PMLA was heated from room temperature up to temperatures above T_i and then cooled to the initial temperature is depicted in Figure 10. The reminiscent spherulitic texture present in the initial sample (Figure 10a) changed into a kind of focal conic texture texture characteristic of a smectic mesophase, likely of A-type, upon heating above T_m. This texture vanished and all signs of birrefringence disappeared upon

heating above T_i. Upon cooling the smectic structure was readily recovered, and finally, crystallization took place generating well developed spherulites. A detailed and repeated inspection of the melting process under the POM did not revealed differences between the first and second heating which relate side chain melting with the endotherm observed at 100 °C. In the case of 14ATMA·PMLA, the smectic phase is already present at room temperature, and it undergoes the same pattern of changes as do the higher members of the series (Figure 11). In this case, however, the melting-crystallization process is not observable since the alkyl side chain is not long enough as to form stable crystallites in these complexes.

Concluding Remarks

Stoichiometric or nearly stoichiometric complexes of microbial poly(malic acid) and cationic surfactants can be readily prepared by a simple mixing-precipitation procedure in aqueous medium. The complexes have a comblike architecture and are insoluble in water but soluble in nonpolar or polar aprotic solvents. In the solid state, they all adopt a biphasic arrangement in which the paraffinic and polyester nanophases are clearly segregated to form an amphiphilic structure ordered on the nanometric scale. The alkyl side chain with 16 to 22 carbon atoms are crystallized at temperatures and melt at temperatures between 30 and 70 °C. After melting, the complexes adopt a smectic structure that become isotropic upon heating above 100 °C. Both melting and isotropization are reversible processes that occur far below the decomposition temperature.

Acknowledgment. We thank the CICYT (Comisión Interministerial de Ciencia y Tecnología) of Spain for financial support (Grant MAT2003-06955-C02) and the CONACYT (México) for the Ph.D. grant awarded to J.A. Portilla-Arias.

References and Notes

(1) Tomalia, D. A.; Wang, Z. G.; Tirrell, M. *Curr. Opin. Colloid. Interface Sci.* **1999**, *4*, 3.
(2) Loos, K.; Muñoz-Guerra, S. Microstructure and crystallization of rigid coil comblike polymers and block copolymers. In *Supramolecular Polymers*, 2nd ed.; Ciferri, A., Ed.; Marcel Dekker: New York, 2005.
(3) (a) Wang, M.; Zhang, G.; Chen, D.; Jiang, M.; Liu, S. *Macromolecules* **2001**, *34*, 7172. (b) Borfanou, K.; Topouza, D.; Sakellaniou, G.; Pispas, S. *J. Polym. Sci., Polym Chem.* **2003**, *41*, 2454. (c) Zhang, Y. W.; Jiang, M.; Zhao, J. X.; Wang, Z. X.; Dou, H. J.; Chen, D. Y. *Langmuir* **2005**, *21*, 1531. (d) Zhang, Y. W.; Jiang, M.; Zhao, J. X.; Ren, X. W.; Chen, D. Y.; Zhang G. Z. *Adv. Funct. Mater.* **2005**, *15*, 695.
(4) Thünemann, A. *Prog. Polym. Sci.* **2002**, *27*, 1473.
(5) Platé, N. A.; Shibaev, V. P. *J. Polym. Sci., Macromol. Rev.* **1974**, *8*, 117.
(6) Antonietti, M.; Conrad, J.; Thünemann, A. *Macromolecules* **1994**, *27*, 6007.
(7) (a) Ponomarenko, E. A.; Waddon, A. J.; Bakeev, K. N.; Tirrell, D. A.; MacKnight, J. *Macromolecules* **1996**, *29*, 4340. (b) Ponomarenko, E. A.; Waddon, A. J.; Tirrell, D. A.; MacKnight, J. *Langmuir* **1996**, *12*, 2169.
(8) (a) Pérez-Camero, G.; García-Alvarez, M.; Martínez de Ilarduya, A.; Fernández, C. E.; Campos, L.; Muñoz-Guerra, S. *Biomacromolecules* **2004**, *5*, 144. (b) García-Alvarez, M.; Alvarez, J. A.; Alla, A.; Martínez de Ilarduya, A.; Herranz, C.; Muñoz-Guerra, S. *Macromol. Biosci*. **2005**, *5*, 30.
(9) Zanuy, D.; Aleman, C. *Langmuir* **2003**, *19*, 3987.
(10) (a) Watanabe, J.; Ono, H.; Uematsu, I.; Abe, A. *Macromolecules* **1985**, *18*, 2141. (b) Iizuka, E.; Abe, K.; Hanabusa, K.; Shirai, H. In *Current Topics in Polymer Science*; Ottembrite, R. M., Ed.; Carl Hanser Verlag: Munich, 1987. (c) Tsujita, Y.; Watanabe, T.; Takizawa, A.; Kinoshita, T. *Polymer* **1991**, *32*, 569. (d) Daly, W. H.; Poche, D.; Negulescu, I. *Prog. Polym. Sci.* **1994**, *19*, 79.
(11) (a) Morillo, M.; Martínez de Ilarduya, A.; Muñoz-Guerra, S. *Macromolecules* **2001**, *34*, 7868. (b) Morillo, M.; Alla, A.; Martínez de Ilarduya, A.; Muñoz-Guerra, S. *Macromolecules* **2003**, *36*, 7567.
(12) Lee, B.-S.; Vert, M.; Holler, E. In *Biopolymers*; Doi, Y., Steinbüchel, A., Eds.; Wiley-VCH: Weinheim, Germany, 2002; Vol. 3, pp 75−103.
(13) Hendrix, W. T.; von Rosenberg, J. L. *J. Am. Chem. Soc.* **1976**, *98*, 4850.
(14) Daniel, J. W.; Baldwin, H. H. In *Methods in Cell Physiology*; Presscott, D. A., Ed.; Academic Press: London, 1964; pp 9−41.
(15) Holler, E. In *Handbook of Engineering Polymeric Materials*; Cheremisinoff, N. P., Ed.; Marcel Dekker: New York, 1997; pp 93−103.
(16) Bergmeyer, H. U. *Methoden der Enzymatischen Analyse*; Verlag Chemie: Weinheim, Germany, 1974; pp 1632−1639.
(17) Fernández, C. E.; Mancera, M.; Holler, E.; Bou, J.; Galbis, J. A.; Muñoz-Guerra, S. *Macromol. Biosci.* **2005**, *5*, 172.
(18) Tsiourvas, D.; Paleos, C. M.; Skoulios, A. *Macromolecules* **1997**, *30*, 7191.
(19) Flory, P. J.; Vrij, A. *J. Am. Chem. Soc.* **1963**, *85*, 3548.
(20) (a) Jordan, E. F., Jr.; Feldeisen, D. W.; Wrielev, A. N. J. *Polym. Sci., Part A-1* **1971**, *9*, 1835. (b) Jordan, E. F., Jr.; Artymyshyn, B.; Speca, A.; Wrigley, A. N. J. *Polym. Sci. Part A-1* **1971**, *9*, 3349.
(21) Broadhurst, M. G. *J. Res. Natl. Bur. Stand., Sect. A* **1962**, *66A*, 241.
(22) Thünemann, A. F.; General, S. *Langmuir* **2002**, *16*, 9634.
(23) López-Carrasquero, F.; Montserrat, S.; Martínez de Ilarduya, A.; Muñoz-Guerra, S. *Macromolecules* **1995**, *28*, 5535.

BM050490T